HNOTE 866-V2

Λ Acceptance/Efficiency as functions of x_F and p_t^2

Jürgen Engelfried, E. Alejandro Blanco-Covarrubias, José Luis Sánchez
Instituto de Física
Universidad Autónoma de San Luis Potosí, Mexico

April 2006

Abstract

We run a high statistic Monte Carlo (embedding) study to obtain the Λ acceptance and reconstruction efficiency as a function of x_F and p_t^2, for the different targets Contrary to earlier studies we conclude that especially at low x_F and/or high p_t both kinematic variables have to be taken into account simultaneously. As final results we obtain an analytical model (a 2 dimensional function) describing the efficiency.

1 Introduction

In earlier production studies we always assumed that the acceptance is independent of p_t, which makes it only necessary to correct in x_F. For our studies using Λ's, we found that this is not true at low x_F and/or high p_t.

We require a good acceptance corrections for studies related to the back-splash of the first copper target [1], the Λ production and asymmetry [2, 3], and the Λ polarization [4].

This makes it necessary to correct in both variables at the same time, in addition to consider in which target the primary interaction occurred, increasing enormously the needed statistics. We ran about $2.4 \cdot 10^9$ embedded events, still not enough to obtain smooth acceptance functions.

To overcome this problem, we parametrize the acceptance function and obtain an analytic expression.

We use as basic variables for this study the longitudinal (p_l) and transverse (p_t^2) momentum components of the Λ. Even though for production studies we will calculate x_F, for the acceptance p_l is the more basic variable and is independent of the beam particle.

2 Producing the events with EDG

We use EDG to produce the events. We produced $2.4 \cdot 10^9$ events with parameters $x = 1$ and $b = 1$. With this, the events follow $(1 - x_F)^1$ and a Gaussian in p_t with $\sigma = 1\,\mathrm{GeV}/c$. From these original events, we removed all Λ's which had a decay length of more than 30 cm. These will anyway not be reconstructed, and we save about a factor 100 in computing time.

3 Embedding and Reconstructing the Λ's with *soap*

We used standard *soap*, with *pass2.tseg*, with standard embedding. The primary interactions are about equally distributed within the five charm targets, with a small fraction of interactions in the scintillators (taken into account later). As underlying events we use randomly selected files from run 10783 (1million). Λ's are reconstructed within the *recon* package, using *v2*, and a cut $L/\sigma > 5$. The proton has to be identified with standard criteria in the RICH. For the candidates, we write *vtuple* output.

4 Calculating the Acceptance

For 20 bins in p_l (from 0 to 600 GeV/c) and separately for every charm target we filled two 2-dimensional histogram of p_t^2 versus mass, and performed sideband subtraction to obtain a clean distribution of the reconstructed Λ's as a function of p_t^2. We subtract the distributions for "natural" Λ's contained in the underlying events[1] to obtain the distribution for the reconstructed embedded Λ's. This distribution we divided by the distribution obtained from the original edg events (before removing $z > 30$). For the two histograms we used 25 bins in p_t^2 from 0 to 10 GeV$^2/c^2$ and from 0 to 2 GeV$^2/c^2$ (to increase the precision for low p_t^2 where we have most of our data). We combined the two histograms, obtaining finally five matrices (on per target) with 900 elements each denoting the acceptance in a given (p_l, p_t^2) bin together with the statistical error. A histogram representing the values is shown in fig 1. The statistical fluctuations are still large, we cannot apply this acceptance correction to the real data, which are much smoother.

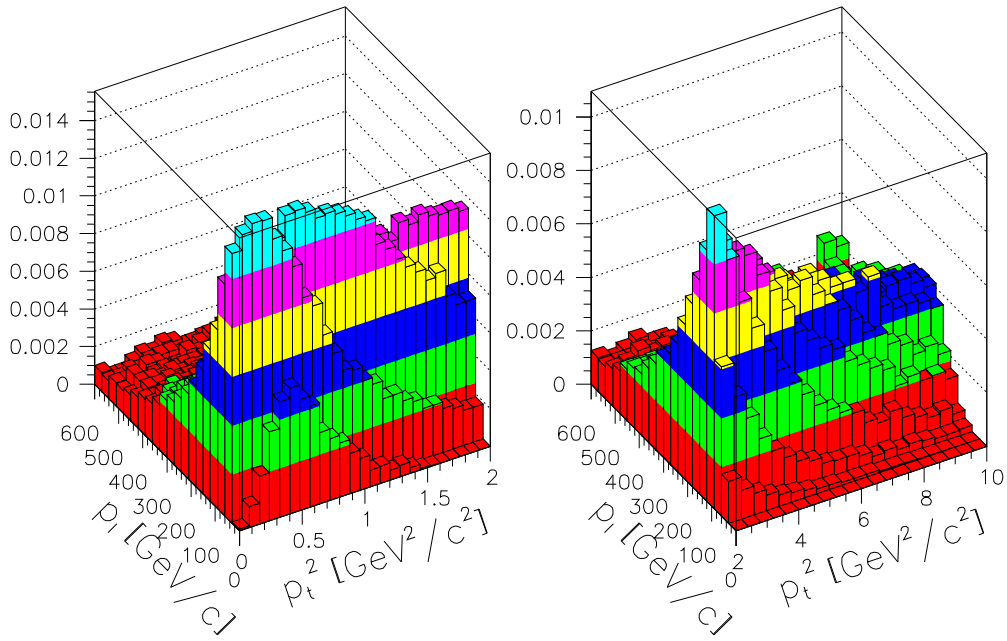

Figure 1: Λ acceptance as a function of p_l and p_t^2 as obtained with our Monte Carlo simulation for target 6 (first copper target).

5 A Model for the Acceptance

For $x_F > 0.2$ or so we see an exponential decrease in the acceptance. We assume that this is due to the long lifetime of the Λ, with only a small fraction decaying before the silicon strip detectors. This fraction decreases with increasing momentum (or increasing x_F) due to time dilation. For a particle with mass M, and lifetime $c\tau$, we obtain [2]

$$\text{Acceptance}(p_l) \approx 1 - \exp\left(-\frac{d}{c\tau\sqrt{\left(\frac{p_l}{Mc^2}\right)^2 + 1}}\right) \tag{1}$$

where d is the size of a box where the Λ has to decay to be detected. d depends obviously on the target. At lower x_F and/or higher p_t^2 the acceptance is reduced due to purely geometric effects.

In a first attempt we tried to fit the p_t^2 distributions in bins of p_l, but failed to find a simple function. We switched to the p_l distributions in bins of p_t^2. In figures 2-6 (blue line) we fit to a combined function: at high

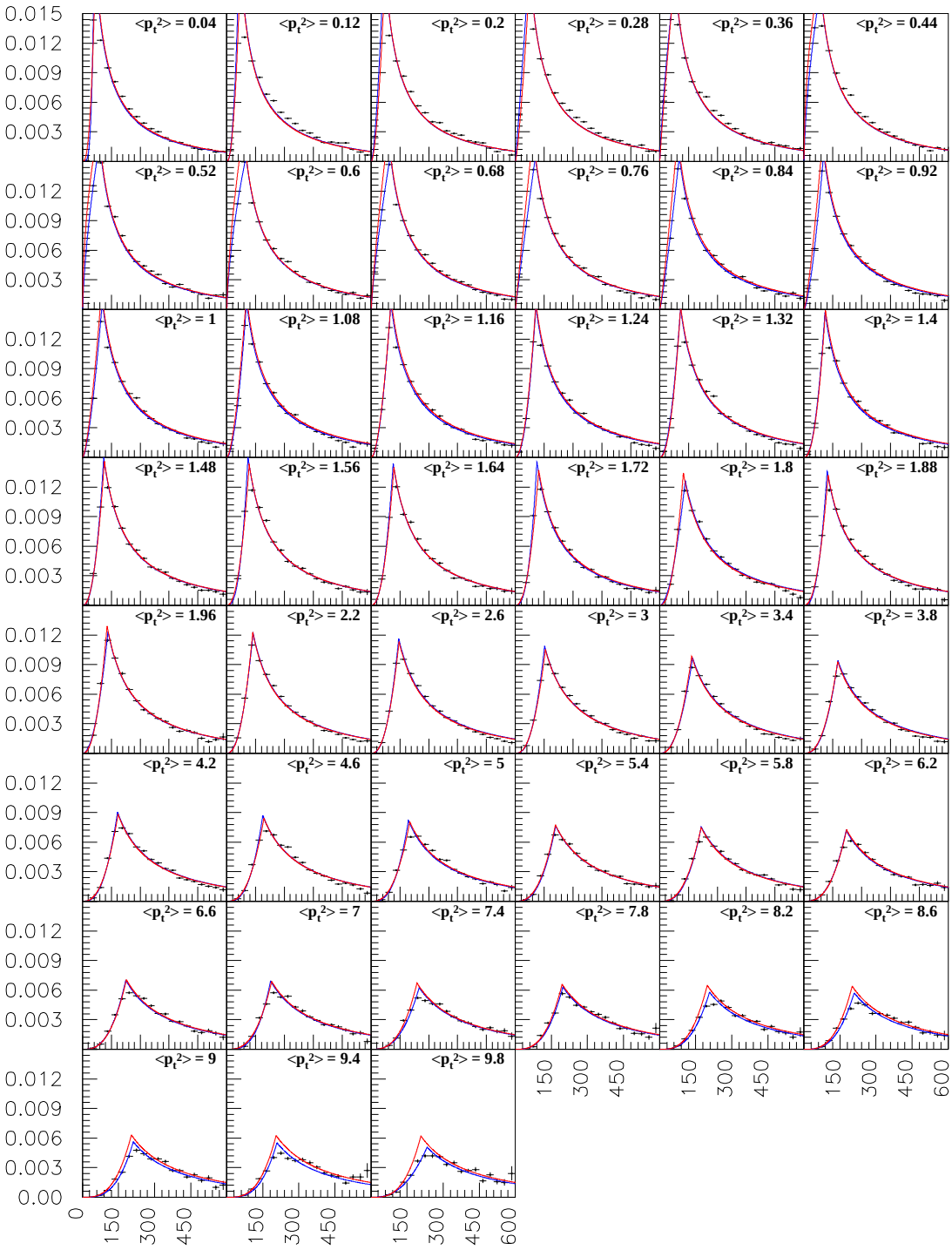

Figure 2: Efficiency as a function of p_l in bins of p_t^2 for target 6. Points: Results from EDG-Embedding. Blue lines: fits with function described in text. Red lines: Efficiencies with final two-dimensional function (equation 2) describing the efficiency.

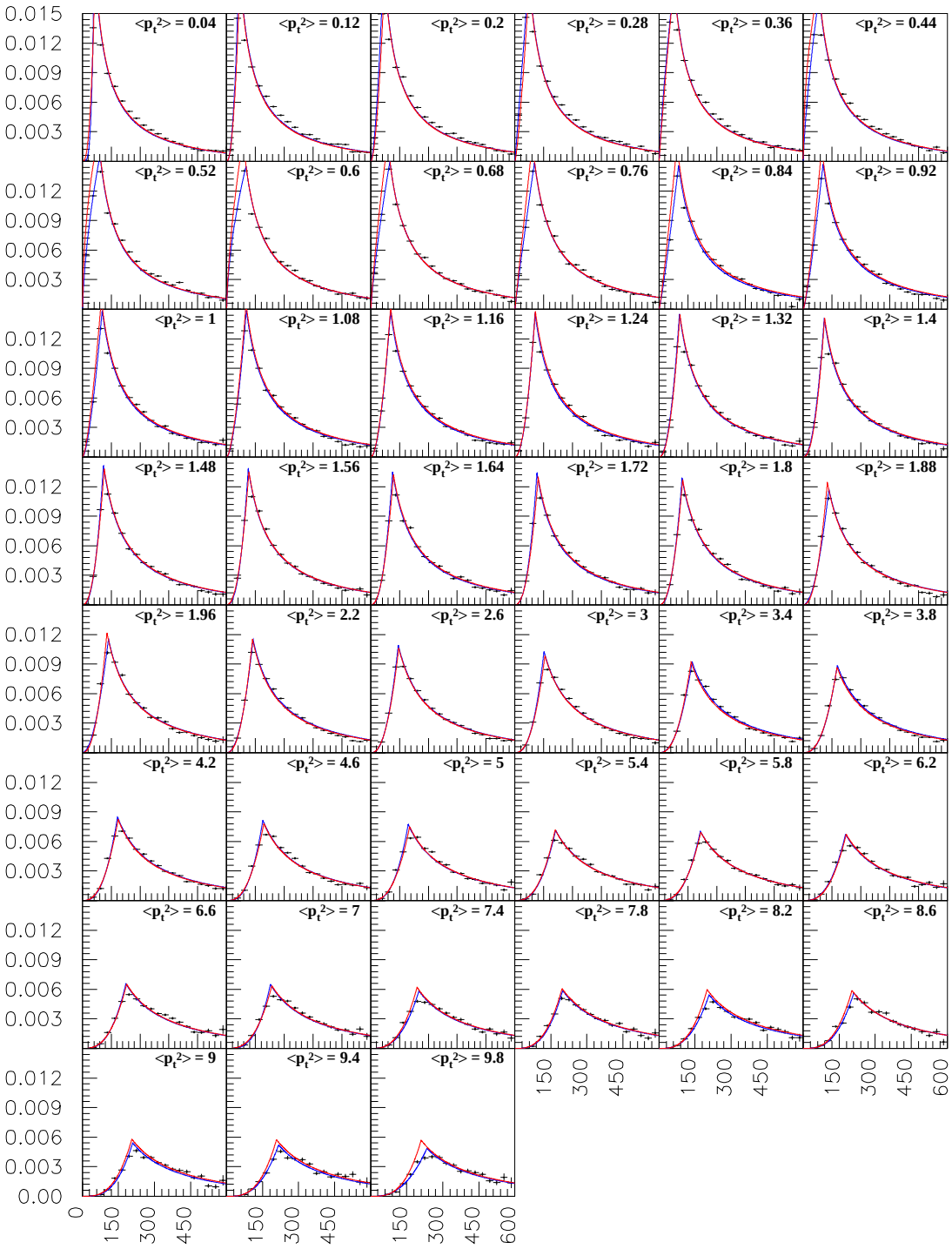

Figure 3: Efficiency as a function of p_l in bins of p_t^2 for target 7. Points: Results from EDG-Embedding. Blue lines: fits with function described in text. Red lines: Efficiencies with final two-dimensional function (equation 2) describing the efficiency.

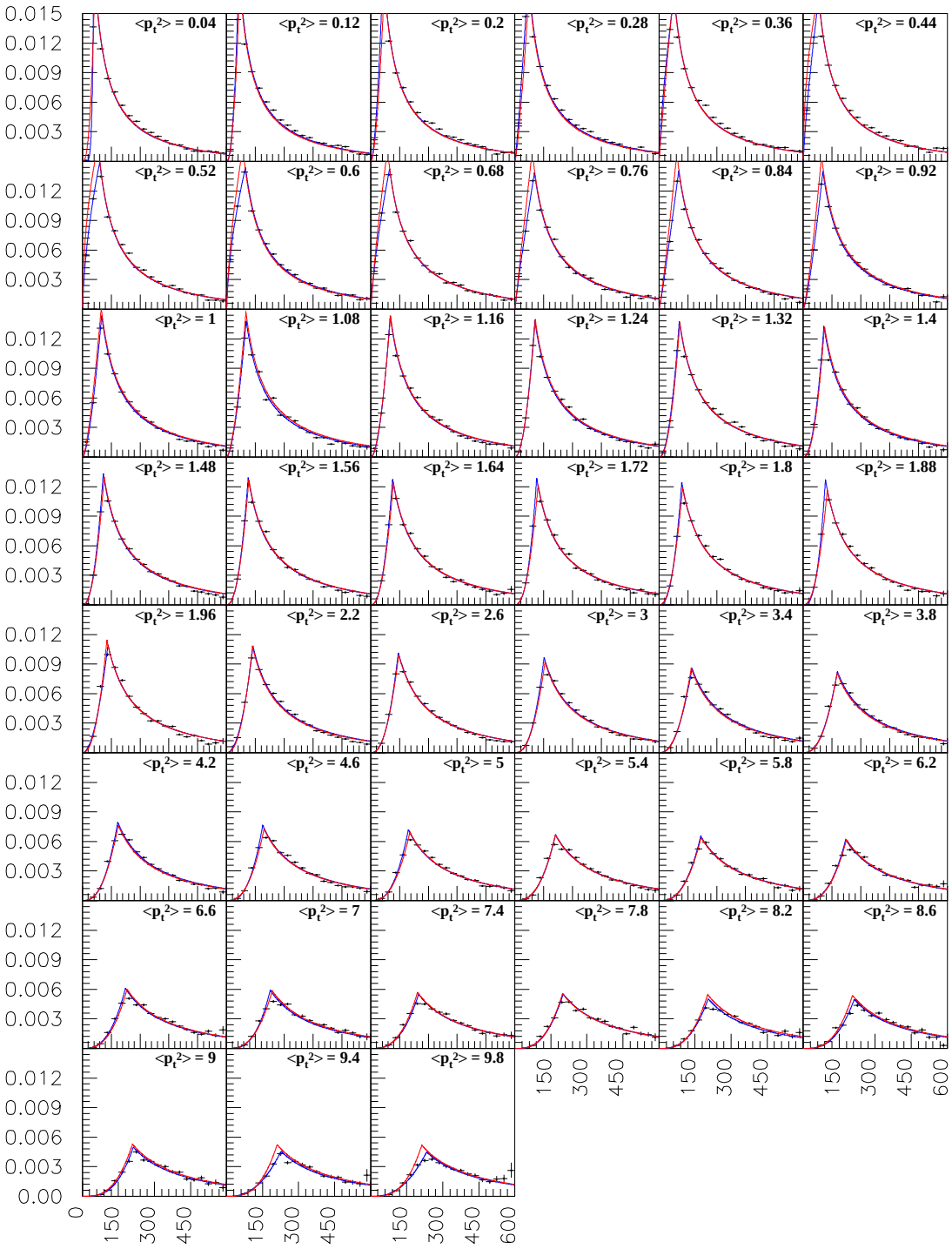

Figure 4: Efficiency as a function of p_l in bins of p_t^2 for target 8. Points: Results from EDG-Embedding. Blue lines: fits with function described in text. Red lines: Efficiencies with final two-dimensional function (equation 2) describing the efficiency.

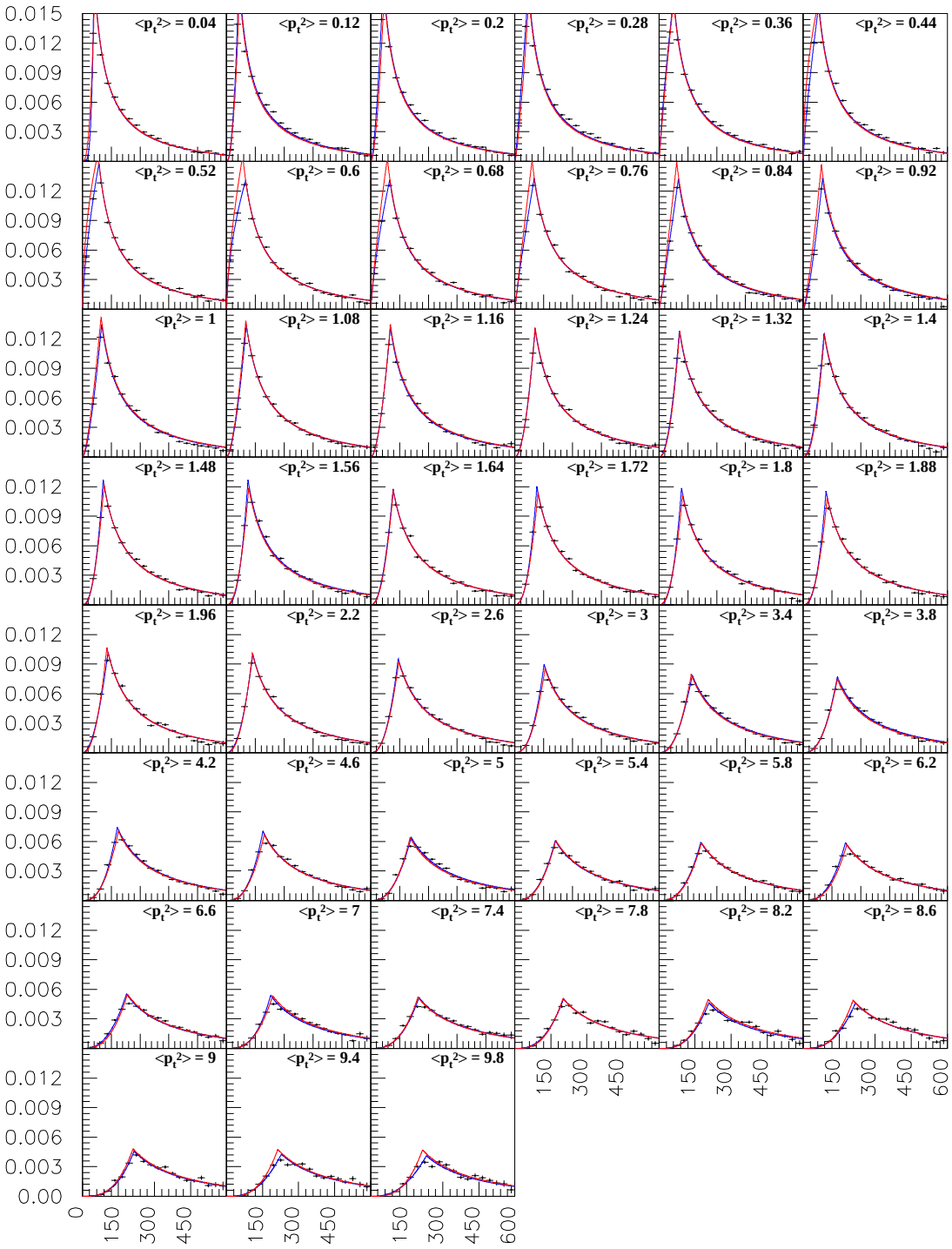

Figure 5: Efficiency as a function of p_l in bins of p_t^2 for target 9. Points: Results from EDG-Embedding. Blue lines: fits with function described in text. Red lines: Efficiencies with final two-dimensional function (equation 2) describing the efficiency.

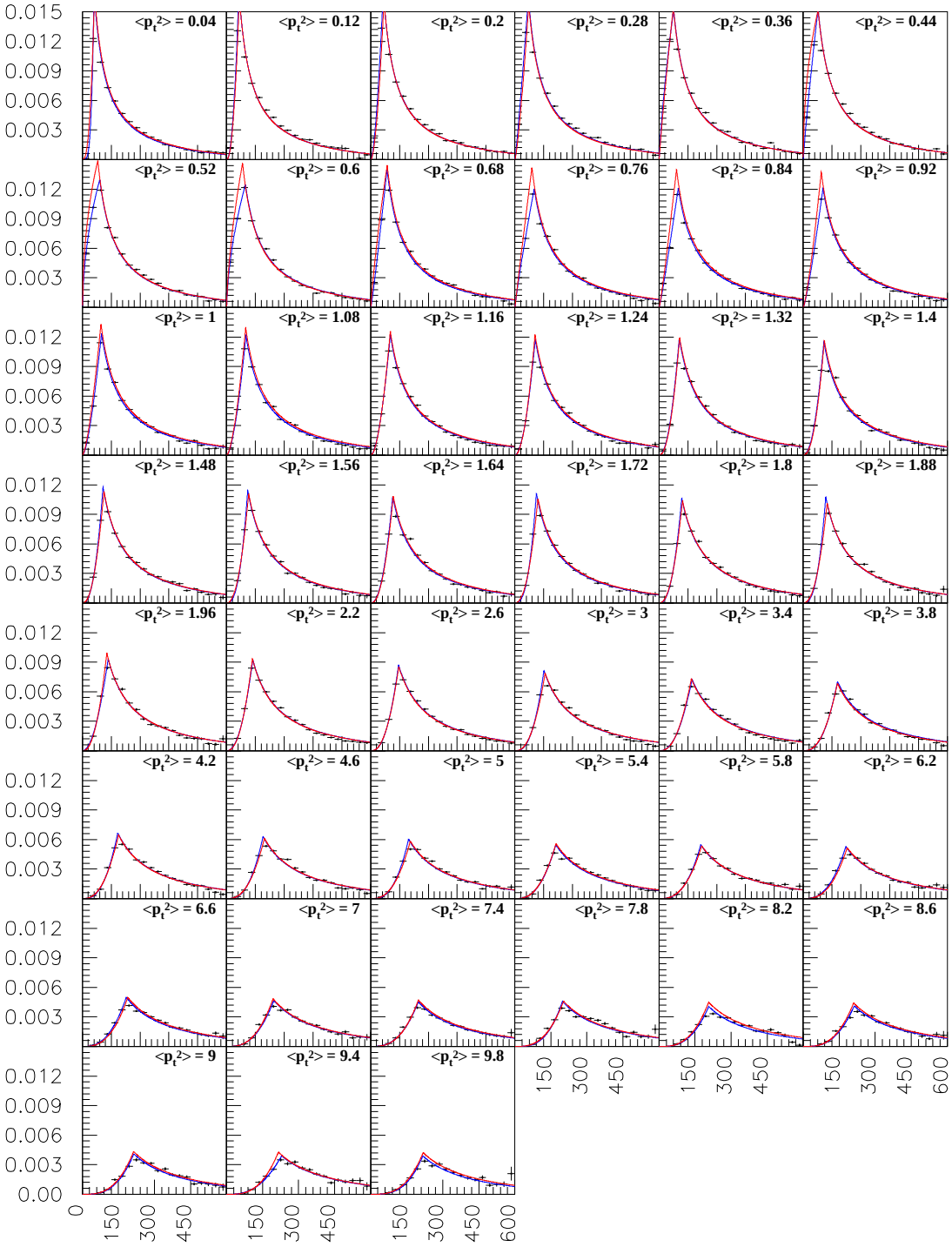

Figure 6: Efficiency as a function of p_l in bins of p_t^2 for target 10. Points: Results from EDG-Embedding. Blue lines: fits with function described in text. Red lines: Efficiencies with final two-dimensional function (equation 2) describing the efficiency.

x_F to equation 1, at low x_F to a power distribution Ap_l^a. The parameter A is eliminated with the condition of continuity at the point where the two functions join. Overall we have four parameters: a renormalization parameter in equation 1 to accommodate for reconstruction losses (the 1 is left free, but see later); the size of the box (d in equation 1); the point where the two functions join; the exponent a in the power law. All fits are performed for the five targets independently.

The first parameter (the normalization) turns out to have a strong anti-correlation with the size of the box (d); after s short study we fix this parameter at a value of 0.999.

The size of the box (parameter d) is shown in fig. 7. The distributions seems to follow a triangular shape, and we perform a fit to it. We would expect that the first three fit parameters decrease by 1.5 cm for each target; this is not the case. The difference between targets is only between 0.44 cm and 0.63 cm. We attribute this to the fact that in the *v2* package secondary interaction vertices in material are ignored.

The third parameter, the position where the power law and the decay exponential meet, is shown in fig. 8. We parametrize the distributions with second-order polynomials; the offset and the linear term show a dependence on the target, the quadratic term seems to be independent of the target.

The forth parameter, the exponent of the power law, is shown in fig. 9.

With the fit results we finally construct a 2dim function describing the acceptance as a function of the longitudinal (p_l) and transversal (p_t^2) momentum for target t ($6 \leq t \leq 10$):

$$\text{Acceptance}(p_l, p_t^2, t) = \begin{cases} Ap_l^{P(4)} & p_l \leq P(3) \\ P(1) - \exp\left(\frac{-P(2)}{7.89\sqrt{(\frac{p_l}{1.115683})^2+1}}\right) & p_l \geq P(3) \end{cases} \tag{2}$$

where

$$A = \frac{P(1) - \exp\left(\frac{-P(2)}{7.89\sqrt{(\frac{p_l}{1.115683})^2+1}}\right)}{(P(3))^{P(4)}} \tag{3}$$

and $P(1) = 0.999$

$$P(2) = \begin{cases} \frac{(p_2-p_1)}{p_4}p_t^2 + p_1 & p_t^2 \leq p_4 \\ \frac{-(p_2-p_3)}{10-p_4}p_t^2 + p_2 - \frac{-(p_2-p_3)}{10-p_4}p_4 & p_t^2 \geq p_4 \end{cases} \tag{4}$$

with $p_1 = 10.79 - 0.437t$, $p_2 = 13.5 - 0.56t$, $p_3 = 14.4 - 0.63t$ $p_4 = 0.888$.
$P(3) = 58.8 - 0.93t + (25.3 + 0.38t)p_t^2 - 1.21(p_t^2)^2$, and

$$P(4) = \begin{cases} \frac{(p_5-p_9)}{p_{10}}p_t^2 + p_9 & pt^2 \leq p_6 \\ \frac{p_6-p_5}{p_8-p_{10}}p_t^2 + p_5 - \frac{p_6-p_5}{p_8-p_{10}}p_{10} & p_6 \leq pt^2 \leq p_8 \\ \frac{-(p_6-p_7)}{10.-p_8}p_t^2 + p_6 - \frac{-(p_6-p_7)}{10.-p_8}p_8 & p_t^2 \geq p_8 \end{cases} \tag{5}$$

$p_5 = 1.37$, $p_6 = 3.26$, $p_7 = 4.25$, $p_8 = 1.35$, $p_9 = 3.9$, $p_{10} = 0.46$.

We show the result of equation 2 in fig. 2-6 as red lines, and conclude that there is a very good agreement. Finally we use equation 2 to plot the dependence as a function of p_t^2 in bins of p_l (Fig. 10-14). Also here we find perfect agreement. Please keep in mind that in both figures we plot the function for the mean value of the corresponding bin in p_t^2 or p_l, respectively, and we expect, especially where the function changes rapidly, some deviations.

The acceptance function will be included as a FORTRAN subroutine in the next release of *selex_tools*, under the name *lambda_accep.F*.

Acknowledgment

This work was partially supported by the Department of Public Education (Secretaría de Educación Pública), – Under-secretary of Higher Education and Scientific Research, Office of Higher Education – under contract number 2003-24-001-026.

[1] In run 10783 we find about 5000 Λ's, but with a different x_F distribution than we embed.

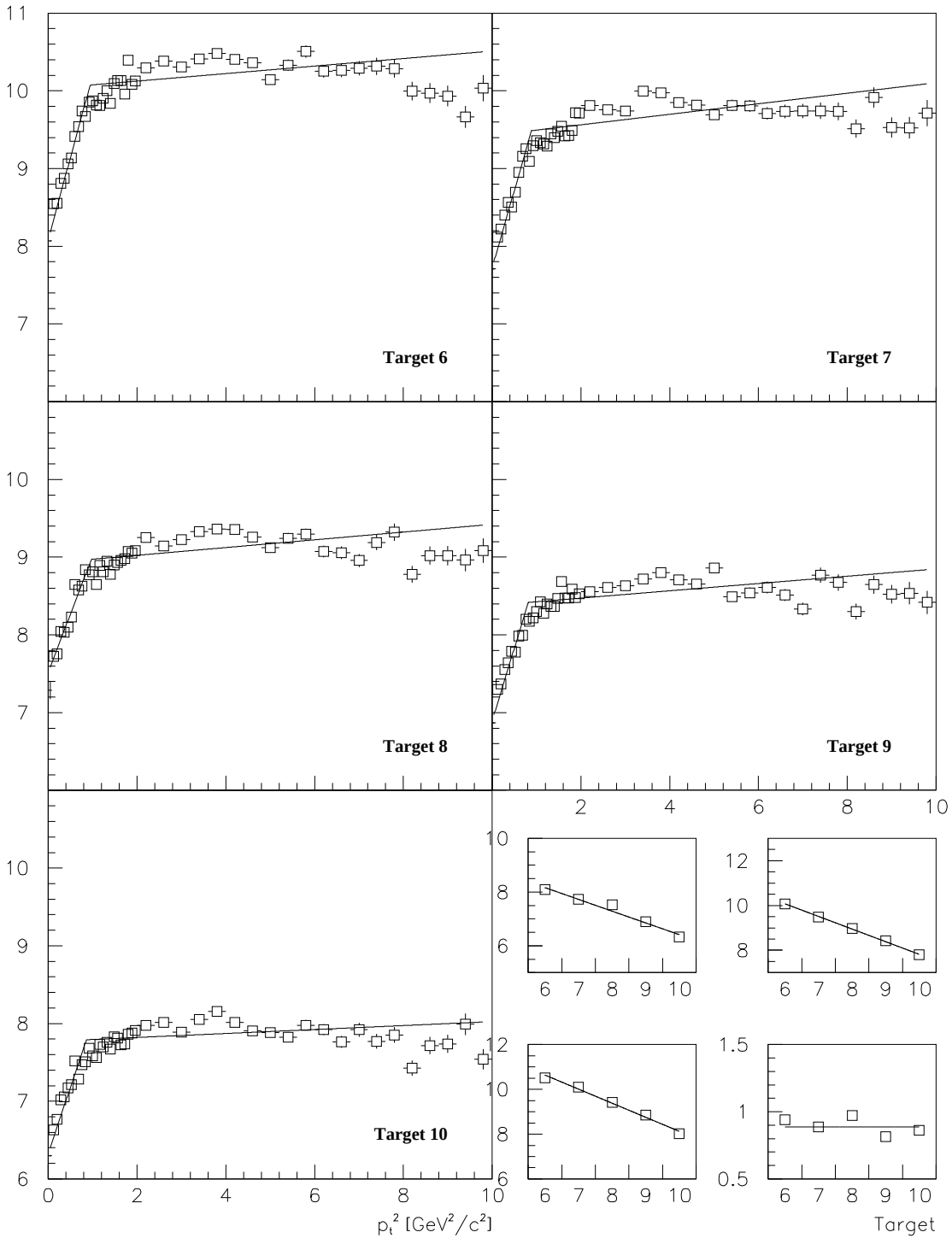

Figure 7: Size of the box (parameter d) as a function of p_t^2 for the five targets. We fit a triangular shape to the distributions. The smaller figures show the distributions of the fit parameter (value at $p_t^2 = 0$, value at maximum, value at $p_t^2 = 10$, position of maximum) for the different targets. Only the position of the maximum seems to be the same for all targets, the other show a linear decrease. For more discussion see text.

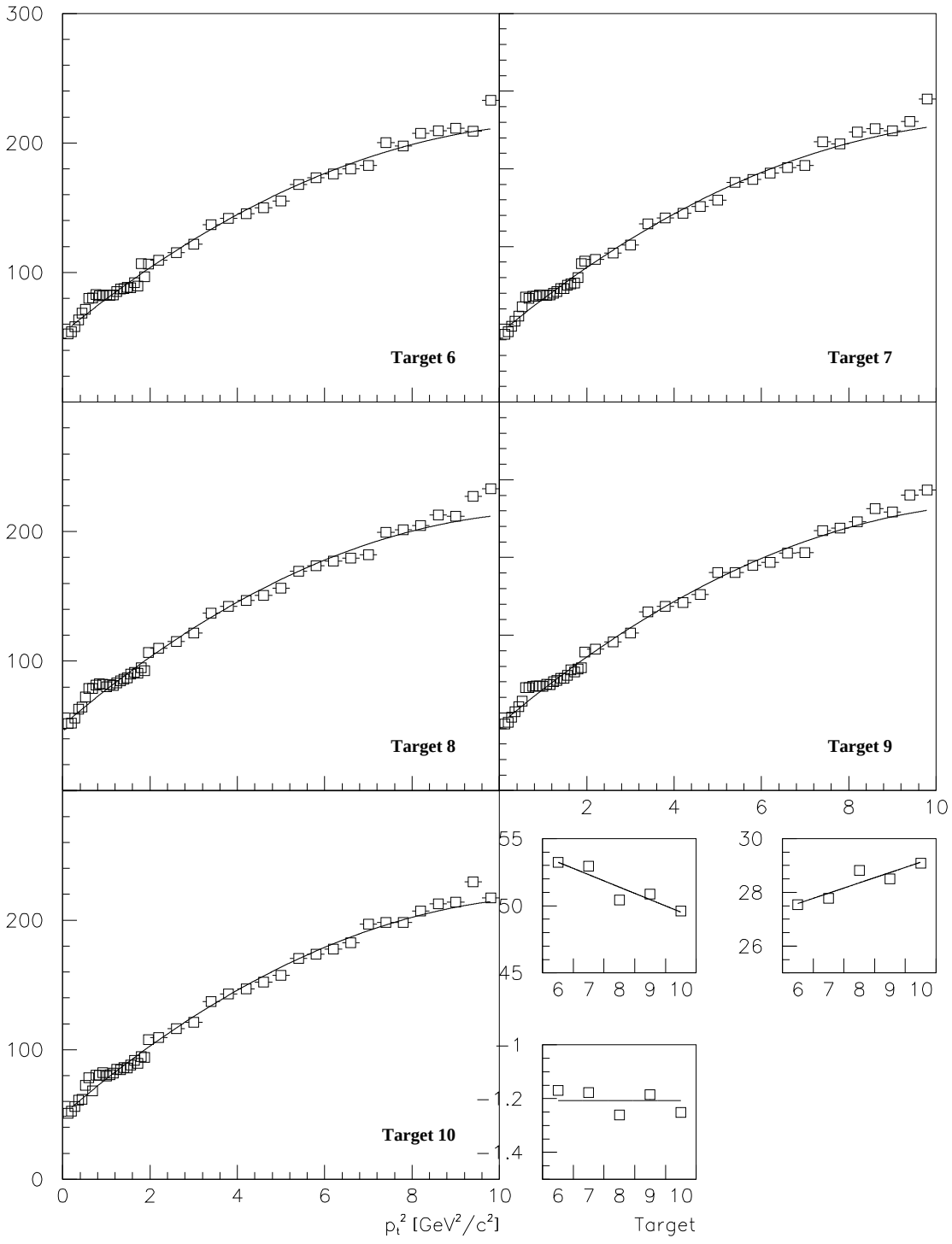

Figure 8: Position where power law a decay exponential meet, as a function of p_t^2 for the five targets. We fit a second-order polynomial to the distributions. The smaller figures show the distributions of the fit parameter (offset, slope, and quadratic term) for the different targets. Only the quadratic term seems to be the same for all targets, the other show a linear dependence.

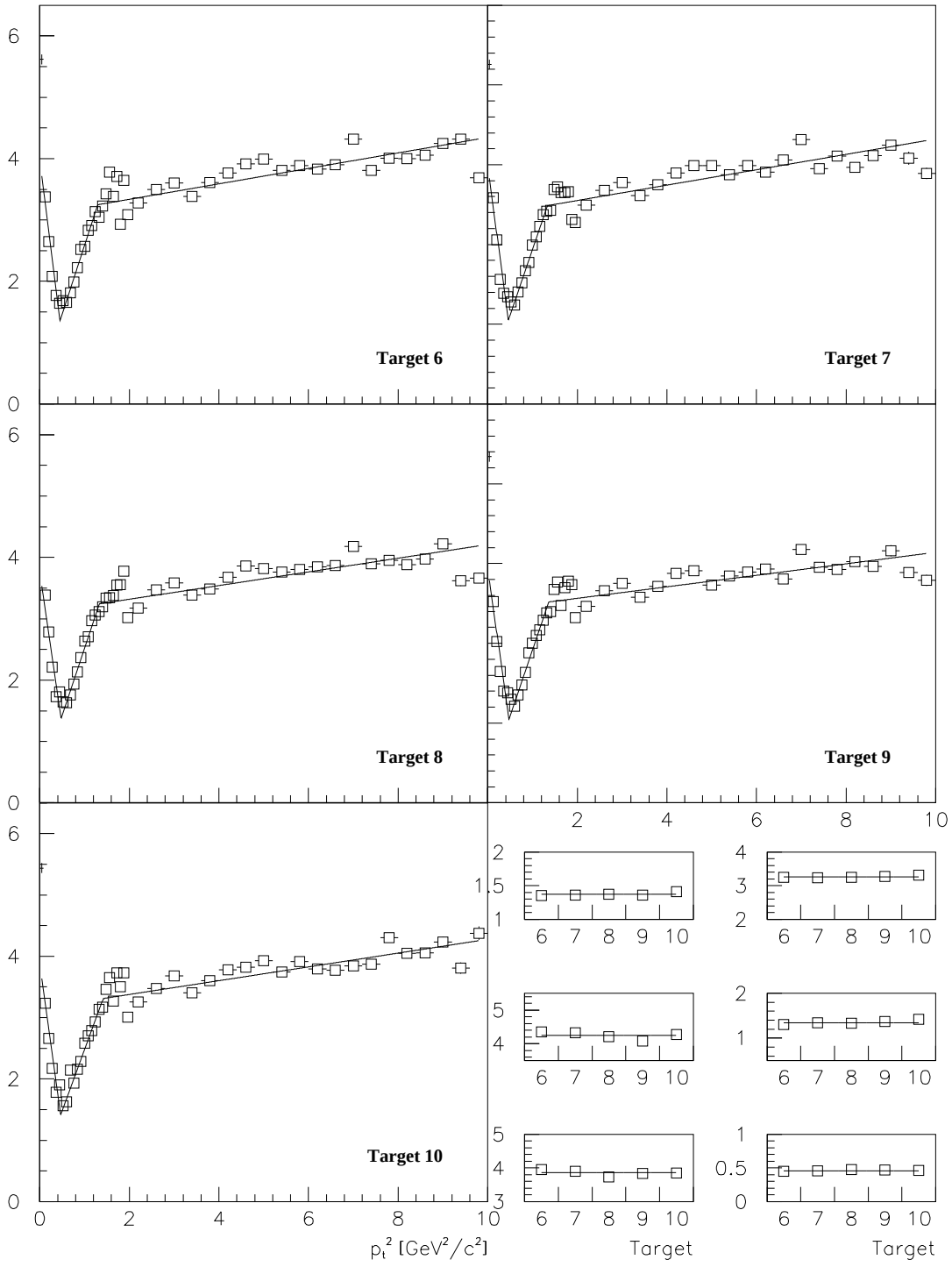

Figure 9: Exponent of the power law as a function of p_t^2 for the five targets. We fit a double-triangular shape with six parameters to the distributions. The smaller figures show the distributions of the fit parameter (value at minimum, value at maximum, value at $p_t^2 = 10$, position of maximum, value at $p_t^2 = 0$, position of minimum) for the different targets. All parameters seem to be independent of the target.

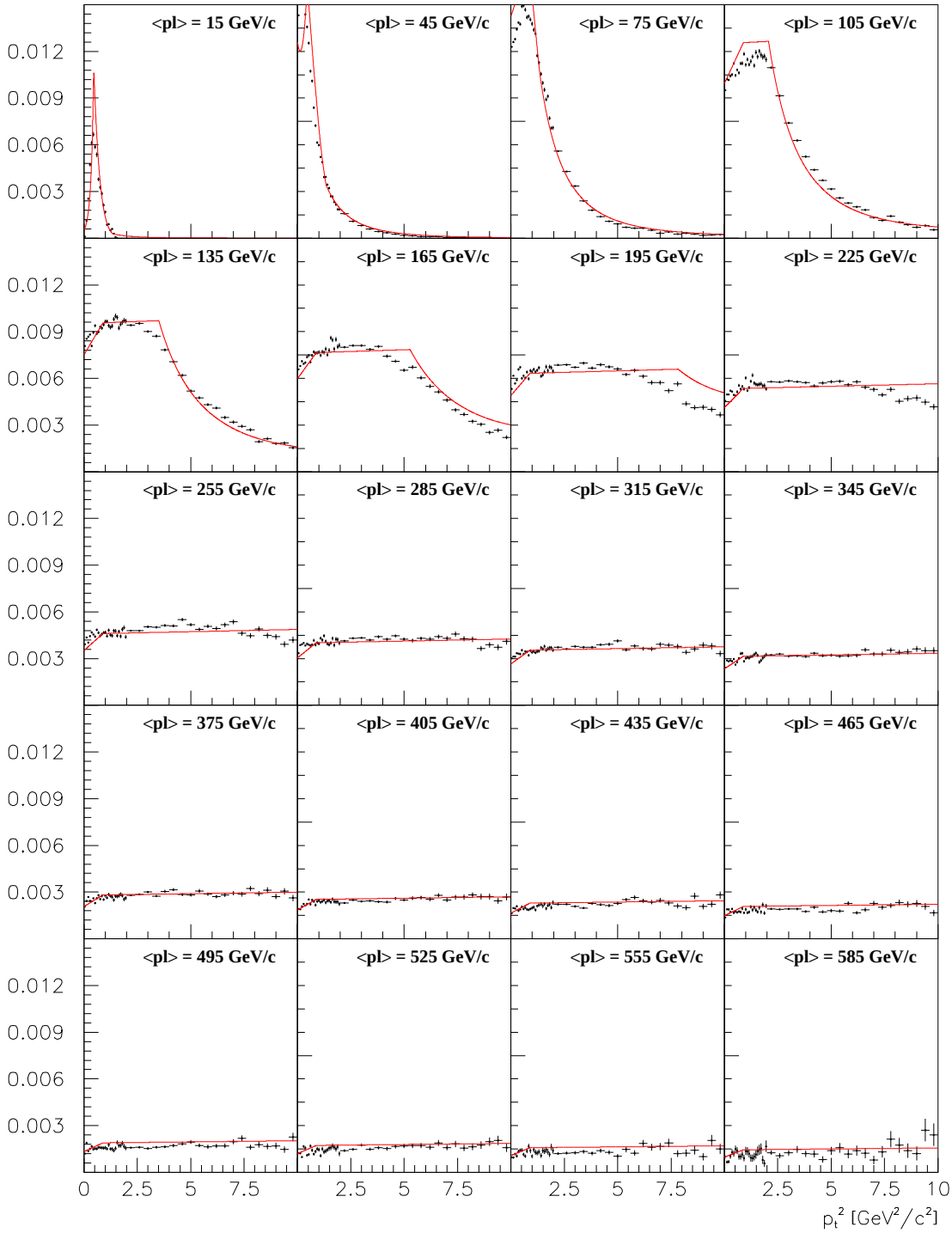

Figure 10: Efficiency as a function of p_t^2 in bins of p_l for target 6. Points: Results from EDG-Embedding. Red lines: Efficiencies with final two-dimensional function (equation 2) describing the efficiency.

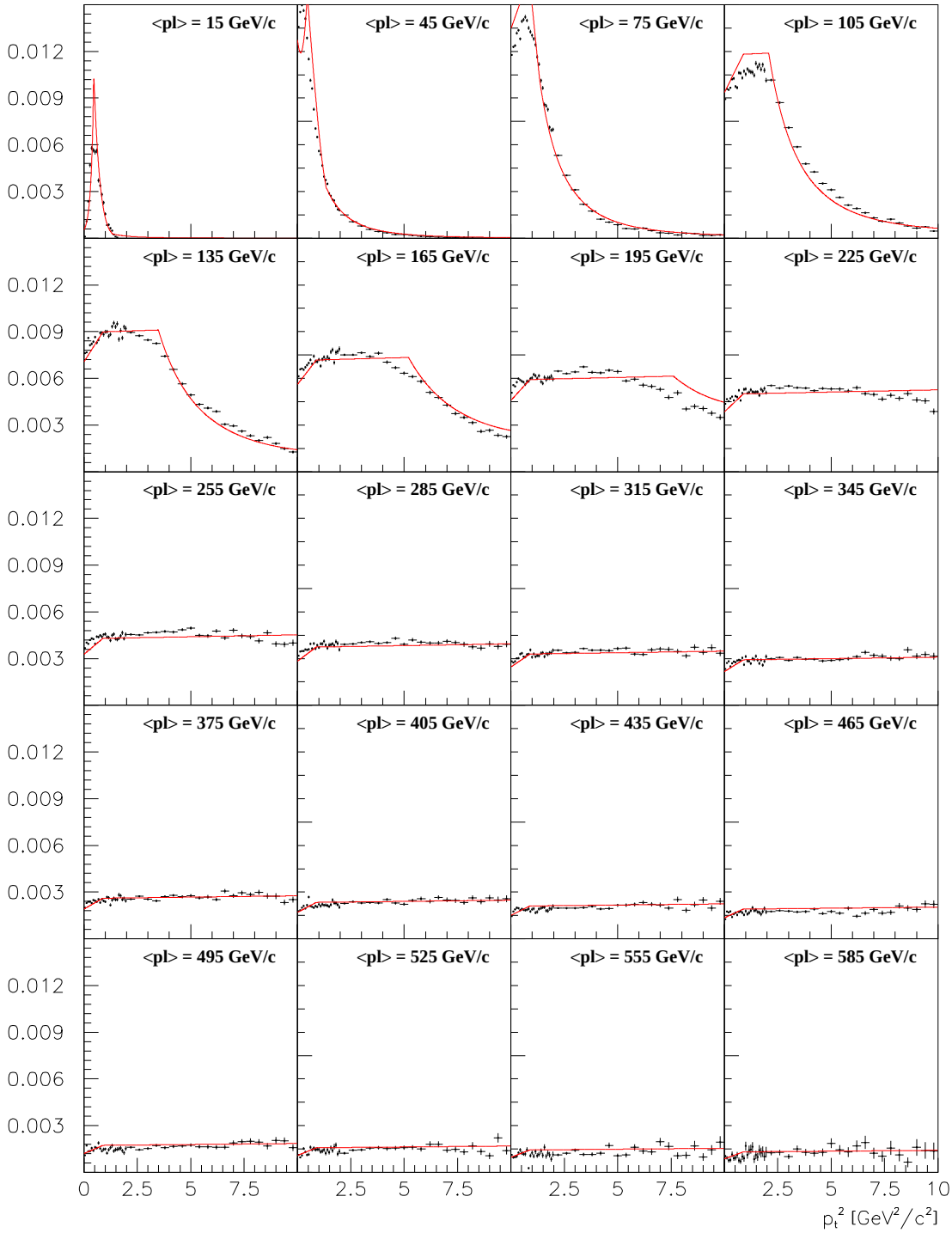

Figure 11: Efficiency as a function of p_t^2 in bins of p_l for target 7. Points: Results from EDG-Embedding. Red lines: Efficiencies with final two-dimensional function (equation 2) describing the efficiency.

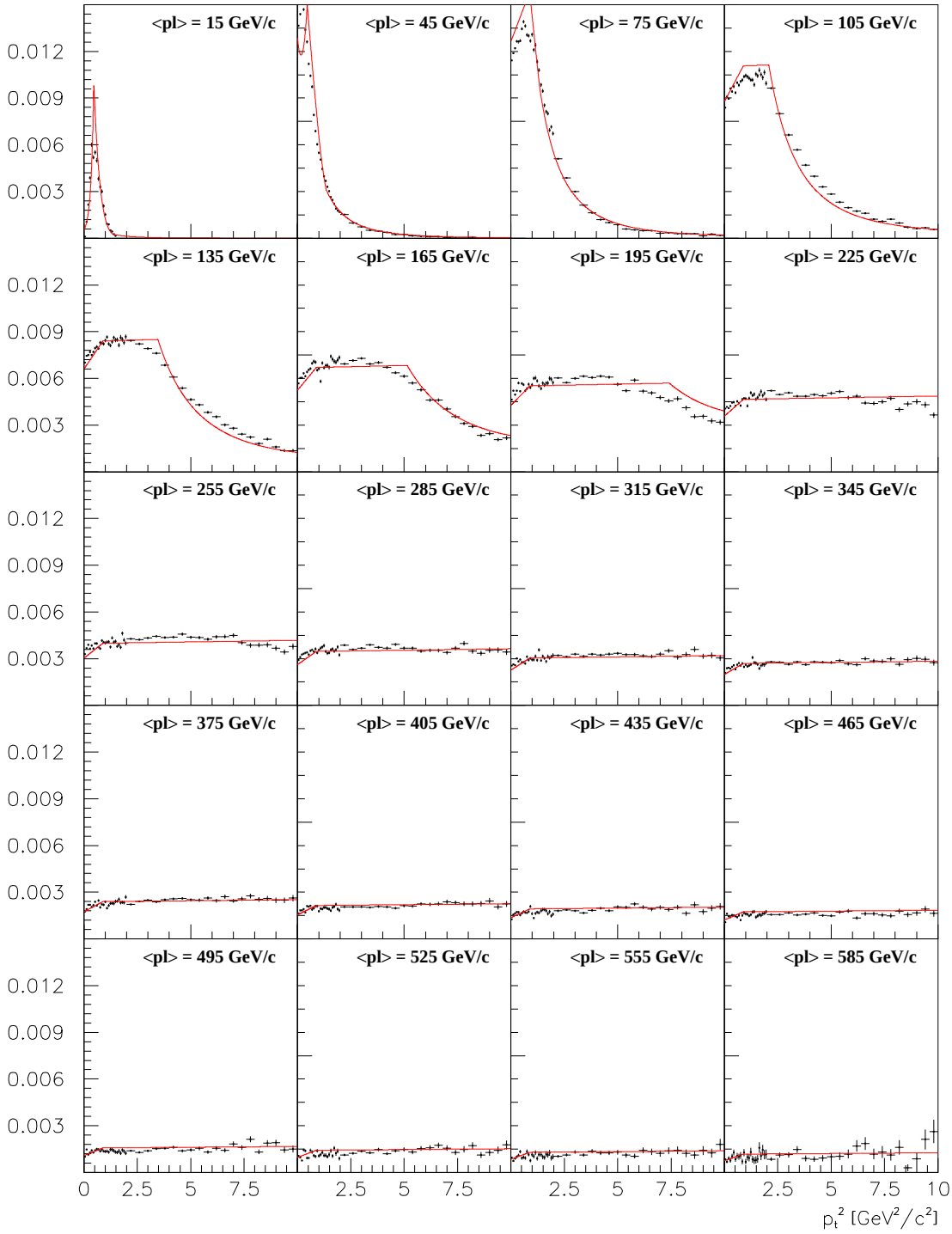

Figure 12: Efficiency as a function of p_t^2 in bins of p_l for target 8. Points: Results from EDG-Embedding. Red lines: Efficiencies with final two-dimensional function (equation 2) describing the efficiency.

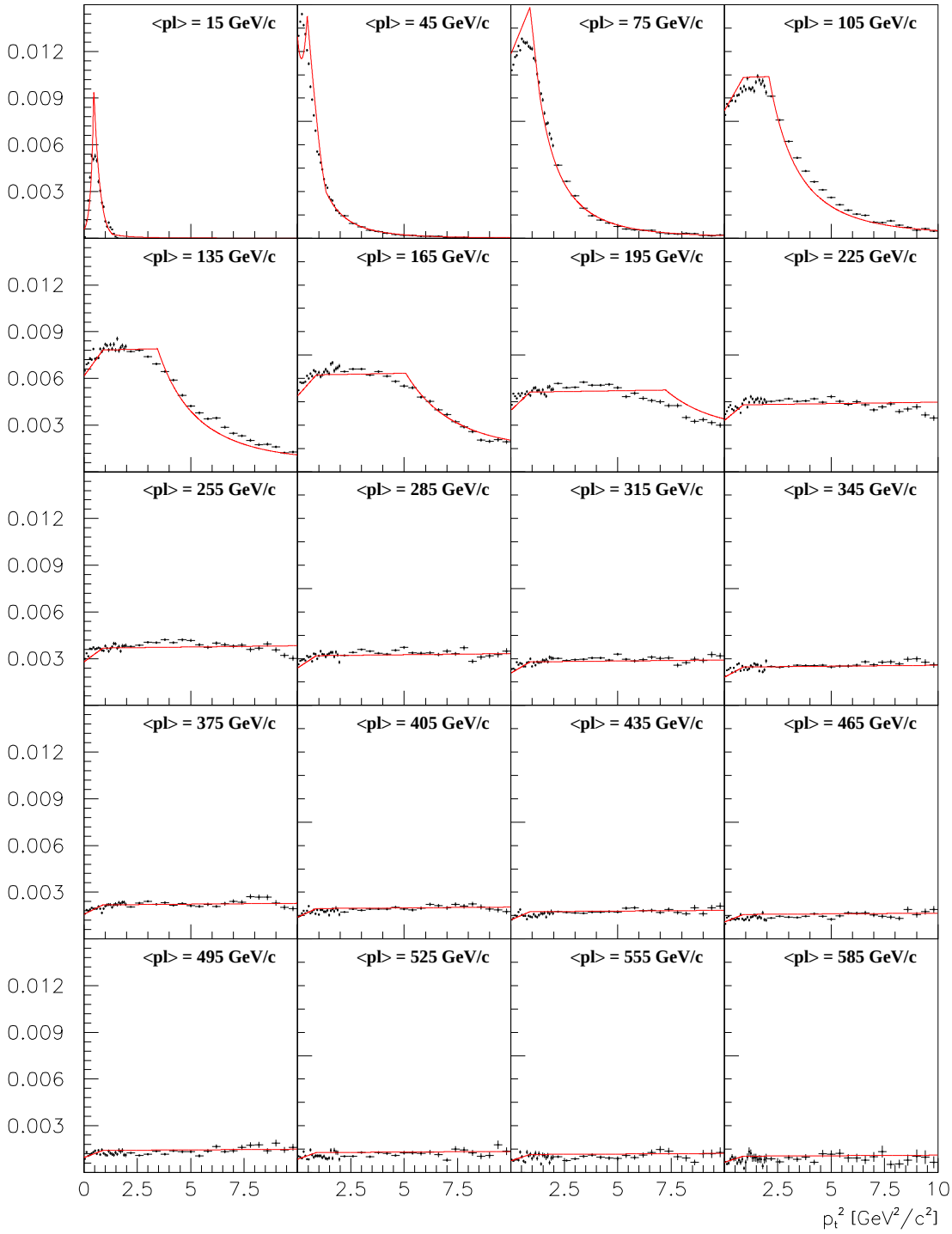

Figure 13: Efficiency as a function of p_t^2 in bins of p_l for target 9. Points: Results from EDG-Embedding. Red lines: Efficiencies with final two-dimensional function (equation 2) describing the efficiency.

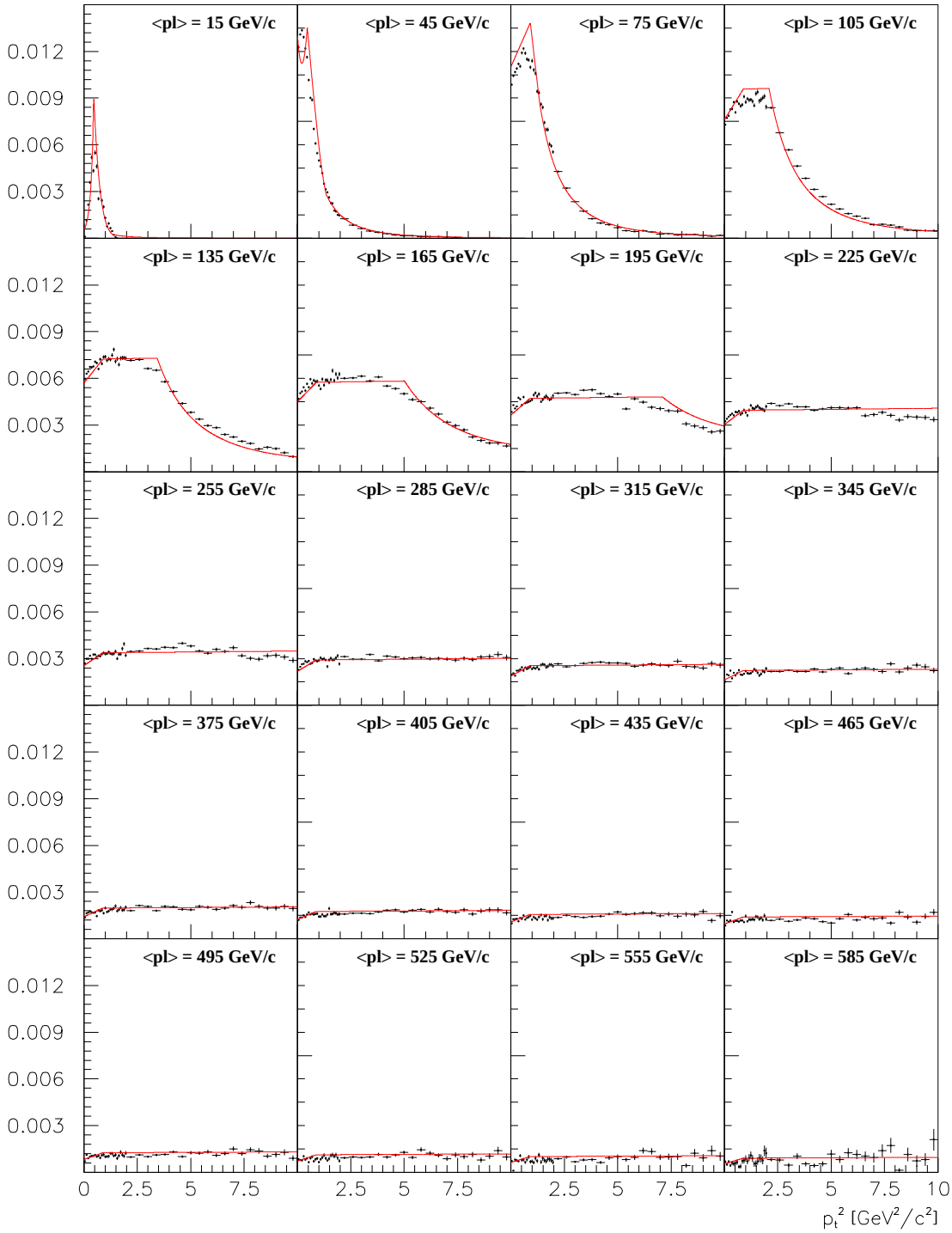

Figure 14: Efficiency as a function of p_t^2 in bins of p_l for target 10. Points: Results from EDG-Embedding. Red lines: Efficiencies with final two-dimensional function (equation 2) describing the efficiency.

References

[1] E.A. Blanco, Ph.D. Thesis (IF-UASLP) and HNOTE in preparation.

[2] M.A. Olivo-Gomez, *Inclusive Production of* Λ, $\bar{\Lambda}$ *and* K_s *in* Σ^-, $\pi^\pm$ *and* p – *Nucleon Collisions* (in Spanish). Master Thesis, Instituto de Física, Universidad Autónoma de San Luis Potosí, December 2004. FERMILAB-MASTERS-2003-05.

[3] J. Engelfried: $\Lambda/\overline{\Lambda}$ *Production and the BTRD.* SELEX Internal Note H-865, February 2006.

[4] J.L. Sanchez, Master Thesis (IF-UASLP) in preparation.